CHEMBIOCHEM

DOI: 10.1002/cbic.200800771

DNA and RNA-Controlled Switching of Protein Kinase Activity

Lars Röglin,[b] Frank Altenbrunn,[a] and Oliver Seitz*[a]

Protein switches use the binding energy gained upon recognition of ligands to modulate the conformation and binding properties of protein segments. We explored whether the programmable nucleic acid mediated recognition might be used to design or mimic constraints that limit the conformational freedom of peptide segments. The aim was to design nucleic acid–peptide conjugates in which the peptide portion of the conjugate would change the affinity for a protein target upon hybridization. This approach was used to control the affinity of a PNA–phosphopeptide conjugate for the signal transduction protein Src kinase, which binds the cognate phosphopeptides in a linear conformation. Peptide–nucleic acid arms were attached to known peptide binders. The chimeric molecules were studied in three modes: 1) as single strands, 2) constrained by intermolecular hybridization (duplex formation) and 3) constrained by intramolecular hybridization (hairpin formation). Of note, duplexes that were designed to accommodate bulged peptide structures (for example, in hairpins or bulges) had lower binding affinities than duplexes in which the peptide was allowed to adopt a more relaxed conformation. Greater than 90-fold differences in binding affinities were observed. It was, thus, feasible to make use of DNA hybridization to reversibly switch from no to almost complete inhibition of Src-SH2–peptide binding, and vice versa. A series of DNA and PNA-based hybridization experiments revealed the importance of charges and conformational effects. Nucleic acid mediated switching was extended to the use of RNA; this enabled a regulation of the enzymatic activity of the Src kinase. The proof-of-principle results demonstrate for the first time that PNA–peptide chimeras can transduce changes of the concentration of a given RNA molecule to changes of the activity of a signal transduction enzyme.

Introduction

Synthetic protein binders have frequently been used to inhibit and study the role of a specific protein–protein recognition event. The binding between two proteins typically involves large interaction interfaces, which can be addressed by synthetic peptides.[1–3] Considerable effort has been invested in order to gain temporal control and switch on or off the bioactivity of the peptide at will.[4–26] In nature, the binding properties of protein segments are frequently regulated through structural reorganization of the protein framework. Such protein switches use the binding energy gained upon a particular recognition event to modulate conformational constraints. We and others explored whether nucleic acid mediated recognition might be used to design or mimic constraints that limit the conformational freedom of peptide segments.[27] This approach requires chimeric molecules that contain both nucleic acid and protein structures. Nucleic acid–peptide conjugates that change affinity for a protein target upon nucleic acid hybridization might offer fascinating opportunities. For example, intracellular RNA molecules might bind to exogenously added nucleic acid–peptide conjugates and interfere with protein–protein interactions. By this, a particular cell-endogenous RNA might be instructed to rewire biological pathways.

The well-established Watson–Crick base-pairing rules provide a guideline for the design of programmed nucleic acid structures and, thus, for the design of constrain elements. This was used to control the activity of guanylate cyclase and protein kinase A.[28–31] The enzymes were equipped with a single-stranded DNA spring that bridged two chosen points of the protein surface. Nucleic acid single strands have a larger persistence length than double strands. Accordingly, formation of a DNA double strandf conferred mechanical stress on the protein, which resulted in changes in the protein activity. Alternative strategies avoid modifications of the protein target in order to allow studies of wild-type proteins.[32,33] Portela and co-workers studied the transcription factor Jun, which is able to form a heterodimer with the transcription factor Fos.[33] The Jun–Fos heterodimer binds duplex DNA in a sequence-specific manner. A DNA single strand was conjugated with a truncated form of Fos, and this construct was unable to bind Jun. However, annealing of a complementary DNA strand activated the DNA–peptide conjugate for binding to Jun. The study showed that DNA hybridization could be used to instruct the formation of inhibitors of protein–DNA interactions.

[a] *F. Altenbrunn,[+] Prof. Dr. O. Seitz*
Department of Chemistry, Humboldt-Universität zu Berlin
Brook-Taylor-Strasse 2, 12489 Berlin (Germany)
Fax: (+49) 30-2093-7266
E-mail: oliver.seitz@chemie.hu-berlin.de

[b] *Dr. L. Röglin[+]*
Department of Biomedical Engineering, Eindhoven University of Technology
De Wielen 8, 5600 MB Eindhoven (The Netherlands)

[+] *These authors contributed equally to this work.*

Supporting information for this article is available on the WWW under http://dx.doi.org/10.1002/cbic.200800771.

WILEY InterScience DISCOVER SOMETHING GREAT

© 2009 Wiley-VCH Verlag GmbH & Co. KGaA, Weinheim

Preliminary work described by us pointed to a potentially generic method for controlling the function of proteins that do not interact with DNA.[32] Our aim was to put peptidic inhibitors of protein–protein interactions under the control of Watson–Crick base pairing. We reckoned that nucleic acid hybridization could introduce constraints in a PNA–peptide hybrid molecule. This approach was used to control the affinity of a PNA–peptide conjugate for the SH2 protein domain of Src kinase, a protein that does not contain a dedicated DNA-binding site. The previous study was focused on the use of DNA hybridization. Only a limited set of intermolecular constrain modes was investigated. We herein present a series of DNA and PNA-based hybridization constraints in intra- and intermolecular formats and demonstrate both increases and decreases of inhibitory activity. Furthermore, we show that hybridization with in vitro transcribed RNA molecules can be used to exert control. It is demonstrated for the first time that RNA-based switching of the binding affinity of a peptide can be used to regulate the activity of a key enzyme of cellular signal transduction, the tyrosine-specific protein kinase Src. Thus, this study suggests that it might be feasible to reassign the function of RNA by using PNA–peptide hybrid molecules.

Results and Discussion

Design of PNA–peptide hybrids that respond to nucleic acid hybridization

Our aim was to design nucleic acid–peptide conjugates in which the peptide portion of the conjugate would experience altered constraints and changes of the affinity for a protein target upon hybridization. We chose peptide nucleic acids (PNA) as DNA/RNA recognition elements, because of the high biostability and ease of incorporation in solid-phase peptide synthesis.[34] Accordingly, the peptide of interest was equipped with two noncomplementary PNA segments (Figure 1). The single-stranded hybrid molecule **I** might adopt a random-coil-like conformation or might have the features of a collapsed structure in which the exposure of hydrophobic nucleobases to water is minimized.[35,36] It was expected that binding of complementary DNA or RNA to the PNA arms would alter the constraints on the peptide structure. For example, seamless hybridization of both PNA arms might induce the loop-like structure in **II**. Alternatively, binding to only one PNA arm or simultaneous hybridization of both PNA arms with DNA that contain unpaired spacer nucleotides between the two cognate sequences might increase the tendency to adopt extended conformations in architectures such as **III** and **IV**.

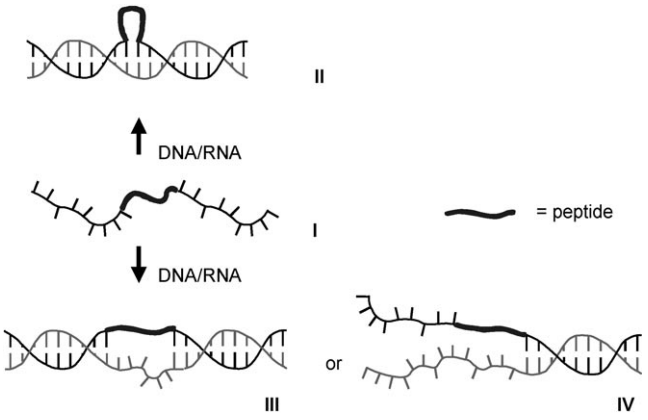

Figure 1. Constraining nucleic acid–peptide conjugates (**I**) by hybridization. The peptide (bold line) experiences different constraints in duplexes that are formed upon seamless base pairing (**II**), simultaneous hybridization of both (**III**) arms, or hybridization of one arm (**IV**) with DNA or RNA that contain unpaired nucleotides.

The PNA–peptide hybrids were directed against the SH2 domain of the Src kinase, an enzyme that triggers phosphorylation cascades.[37–39] The Src kinase exists in active and inactive states. In the inactive state the SH2 domain binds to an internal phosphotyrosine (pTyr)-containing peptide segment located at the C terminus of the kinase.[40–42] Phosphotyrosine-containing peptides or other small molecules that bind to the SH2 domain disrupt the intramolecular interaction and can thereby activate the kinase.[43] The crystal structure of the known high-affinity binding peptide Glu-Pro-Gln-pTyr-Glu-Glu-Ile-Tyr-Leu (consensus motif underlined) in complex with the Src SH2 domain revealed that the peptide is bound in a linear conformation.[44] Thus, it should be feasible to decrease the binding affinity of a phosphopeptide ligand by inducing a bent conformation or, alternatively, to increase the binding affinity by enhancing the tendency to adopt the extended conformation.

Optimization of peptide length and sequence

The objective was to identify a PNA–phosphopeptide hybrid that had high affinity for Src-SH2 in one state and low affinity in another state. We varied the length and sequence of the recognized phosphopeptide. The synthesis of PNA–phosphopeptide hybrids was performed by using automated Fmoc-based solid-phase synthesis (Supporting Information). Three different architectures were analyzed, the single-stranded conjugates **1**–**14a**, the duplex-constrained conjugates **1**–**14b** and conjugates **1**–**14c**, which are constrained by intramolecular hybridization (Table 1). The short peptides **15a** and **16**, and the disulfide-bridged cyclopeptide **15c** were included in the testing to explore the range of affinities that are achieved by covalent constraints. In the initial experiments, PNA–PNA hybridization was used owing to the high stability of the formed PNA–PNA duplexes.[45] The affinity of the PNA–phosphopeptide hybrids for Src-SH2 was assessed by adapting a fluorescence polarization assay that was developed by Lynch and co-workers (Figure S1).[46]

The first set of chimeric molecules (**1**–**10**) was derived from the sequence around the central pTyr-Glu-Glu-Ile motif (Glu-Pro-Gln-pTyr-Glu-Glu-Ile-Pro-Ile-Tyr) found in the Src-SH2 binding hamster middle T antigen (hmT) (Table 1).[47] The others were based on the high-affinity peptides **11** and **12** identified by Charifson and co-workers[48] and the multiphosphorylated peptides **13** and **14**, which were the most potent binders in the study performed by Gilmer and co-workers.[49] The hybrid molecules exhibited different susceptibilities to hybridization-

 © 2009 Wiley-VCH Verlag GmbH & Co. KGaA, Weinheim

Table 1. Dissociation constants K_d [μM] measured for complexes of the Src-SH2 protein and fluorescently labeled PNA–peptide hybrids[a] and peptides in relaxed form (**1**–**14a**, **15a** and **16**) and after constraints introduced by intermolecular (**1**–**14b**) and intramolecular PNA hybridization (**1**–**14c**) or cyclization (**15c**).

	single stranded *N*-FAM-Gly-cgtata-***peptide***-ccaata-Gly-*C*	duplex constrained *N*-FAM-Gly-cgtata-***peptide***-ccaata-Gly-*C* *C*-gcatat—t—ggttat-Ac-*N*	hairpin constrained *N*-FAM-Gly-tattgg-***Peptide*** *C*-ataacc-**e**
PNA–peptide	K_d [μM]	K_d [μM]	K_d [μM]
Glu-Pro-Gln-pTyr-Glu-Glu-Ile-Pro-Ile-Tyr	**1a** 0.3	**1b** 1.8	**1c** 1.4
Glu-Pro-Gln-pTyr-Glu-Glu-Ile-Pro	**2a** 0.3	**2b** 0.7	**2c** 1.6
Pro-Gln-pTyr-Glu-Glu-Ile-Pro-Ile	**3a** 0.7	**3b** 1.5	**3c** 1.6
Gln-pTyr-Glu-Glu-Ile-Pro-Ile-Tyr	**4a** 1.0	**4b** 4.4	**4c** 2.5
Pro-Gln-pTyr-Glu-Glu-Ile	**5a** 0.8	**5b** 5.1	**5c** 3.6
Gln-pTyr-Glu-Glu-Ile-Pro	**6a** 1.0	**6b** 7.9	**6c** 3.4
pTyr-Glu-Glu-Ile-Pro-Ile	**7a** 2.6	**7b** 7.1	**7c** 7.6
Gln-pTyr-Glu-Glu-Ile	**8a** 1.7	**8b** 19	**8c** 25.2
pTyr-Glu-Glu-Ile-Pro	**9a** 1.7	**9b** 6.4	**9c** 2.7
pTyr-Glu-Glu-Ile	**10a** 2.6	**10b** 9.4	**10c** 1.7
Gln-pTyr-Glu-Glu-Ile-Glu	**11a** 1.0	**11b** 3.8	**11c** 1.1
Gln-pTyr-Glu-Glu-Ile-Gln	**12a** 1.7	**12b** 10.3	**12c** 2.1
pTyr-Glu-pTyr-Ile-Glu	**13a** 0.4	**13b** 1.1	**13c** 0.8
pTyr-pTyr-pTyr-Ile-Glu	**14a** 0.5	**14b** 0.9	**14c** 1.2
Peptide			
H-Cys-pTyr-Glu-Glu-Ile-Lys(FAM)-Cys-Gly-NH_2	**15a** 0.1	H-Cys-pTyr-Glu-Glu-Ile-Lys(FAM)-Cys-Gly-NH_2 S—S	**15c** 1.8
FAM-Gly-pTyr-Glu-Glu-Ile-NH_2	**16** 0.3		

[a] PNAs were synthesized as C-terminal amides and are represented in lower-case letters, amino acids are represented in the three letter code. The N- and C-terminal ends of peptides are represented according to IUPAC guidelines, the directionality of PNA conjugates is indicated by marking terminal ends as italicized *N* and *C*.

induced switching of binding affinities. Intermolecular hybridization resulted in two- to eleven-fold decreases of the affinity for the Src-SH2 domain. Hybrid molecule **8** showed the highest responsiveness. After addition of complementary PNA the binding affinity decreased from K_d (**8a**) = 1.7 μM by one order of magnitude to K_d (**8b**) = 19.0 μM. Interestingly, conjugate **8** also proved most responsive to intramolecular hybridization (**8c**), and conferred 15-fold decreases in binding affinity. The melting of the unlabeled hybrid (Ac-tattgg-Gln-pTyr-Glu-Glu-Ile-ccaata-Gly-NH_2, T_m = 73.1 °C) was independent of concentration, as expected for intramolecular base pairing.

Phosphopeptides interact with the Src-SH2 domain predominantly at two distinct positions: the phosphotyrosine-binding pocket and a hydrophobic cavity for the pTyr+3 residue. These two binding pockets are aligned to enable binding of peptides that adopt the extended conformation. Thus, cyclic constraints that involve the main-chain will, in most cases, decrease the tendency to present the pTyr and pTyr+3 side-chains in the required geometry. This is in accordance with most results from inter- and intramolecular hybridization of hybrids **1**–**14**.

It is instructive to compare the results from the PNA–peptide hybrids with binding data from the short peptide **15** in the "relaxed" form, **15a**, and the disulfide-constrained form **15c**. Of note, the 18-fold increase of binding affinity upon reduction of the cyclic peptide **15c** (K_d = 1.8 μM) to the linear peptide **15a** (K_d = 0.1 μM) was in a similar range as the observed difference (15-fold) of the affinity between hairpin-constrained hybrid **8c** and single-stranded **8a**. The affinity of the short "cysteine-free" peptide **16** for the Src-SH2 domain was in a similar range as the affinity of reduced **15a**. Cyclization via disulfide formation has been frequently performed as a means of constraining peptides and used to stabilize turn-like conformations. We assume that hybridization of PNA–peptide–PNA hybrids with nucleic acids can confer similar effects. On the other hand, changes of peptide conformation might not be the only reason for the observed decreases in binding affinity. For example, PNA hybridization might also introduce a steric blockage that affects access of the protein to the recognized peptide motif. Regardless of the mechanism that is involved, the experiments clearly exposed a peptide sequence (Gln-pTyr-Glu-Glu-Ile in **8**) that is amenable to hybridization-based control of the binding activity.

Switching of protein binding affinity by DNA hybridization

The phosphopeptide motif in **8** exhibited the highest PNA-induced change of SH2 affinity. We next investigated the response of **8** to DNA-based hybridization. Initial melting studies exposed negative influences of fluorophores on PNA–DNA hybridization.[50] We therefore chose to explore unlabeled PNA–phosphopeptide hybrids and used a competition assay to assess the affinity of the resulting duplexes for the SH2 protein. In this assay, the PNA–peptide hybrid was titrated to a complex of the Src-SH2 protein and fluorescence-labeled reference peptide **16** (FAM-Gly-pTyr-Glu-Glu-Ile-Ala-NH_2). The fraction of bound **16** was quantified by fluorescence polarization.

 © 2009 Wiley-VCH Verlag GmbH & Co. KGaA, Weinheim

Fitting of the resulting inhibition curves (Figure S3) to a sigmoidal dose–response model with variable slope yielded IC_{50} values.[32] Repeated titration experiments with the unlabeled phosphopeptide **17** (Table 2) revealed IC_{50} values in the low micromolar range ($IC_{50} = 3.3$ μM), which is within reasonable agreement with previously determined affinities for similar peptides (Ac-pTyr-Glu-Glu-Ile, $IC_{50} = 6.5$–8.1 μM).[46,51] The appendage of PNA at the N terminus in hybrid **18** resulted in 4.5-fold enhancements of the SH2 affinity whereas the C-terminal attachment of PNA in **19** induced decreases of binding affinity. Similar effects of terminal substitution have been observed previously.[51]

Table 2. Switching of the affinity of PNA–peptide hybrids for the Src-SH2 protein with DNA and PNA hybridization.

	Peptide conjugates[a]	T_m [°C]	Rel. affintiy[b]
17	Ac-Gln-pTyr-Glu-Glu-Ile-NH_2		1
18	*N*-Gly-Lys-tcgcgtata-Gln-pTyr-Glu-Glu-Ile-Gly_2-*C*	/	4.5
18 d900	*N*-Gly-Lys-tcgcgtata-Gln-pTyr-Glu-Glu-Ile-Gly_2-*C* *3′*-AGCGCATAT-*5′*	34	4.5
18 d960	*N*-Gly-Lys-tcgcgtata-Gln-pTyr-Glu-Glu-Ile-Gly_2-*C* *3′*-AGCGCATATGACTGA-*5′*	43	5.8
19	*N*-Gly_2-Gln-pTyr-Glu-Glu-Ile-ccaatagca-Lys-Gly-*C*	/	0.6
19 d009	*N*-Gly_2-Gln-pTyr-Glu-Glu-Ile-ccaatagca-Lys-Gly-*C* *3′*-GGTTATCGT-*5′*	46	0.6
19 d069	*N*-Gly_2-Gln-pTyr-Glu-Glu-Ile-ccaatagca-Lys-Gly-*C* *3′*-GACTGAGGTTATCGT-*5′*	48	1.7
20	*N*-Gly-Lys-cgcgtata-Gln-pTyr-Glu-Glu-Ile-ccaatagc-Lys-Gly-*C*	/	1.2
20 d900	*N*-Gly-Lys-cgcgtata-Gln-pTyr-Glu-Glu-Ile-ccaatagc-Lys-Gly-*C* *3′*-AGCGCATAT-*5′*	41	1.9
20 d960	*N*-Gly-Lys-cgcgtata-Gln-pTyr-Glu-Glu-Ile-ccaatagc-Lys-Gly-*C* *3′*-AGCGCATATGACTGA-*5′*	46	3.8
20 d009	*N*-Gly-Lys-cgcgtata-Gln-pTyr-Glu-Glu-Ile-ccaatagc-Lys-Gly-*C* *3′*-GGTTATCGT-*5′*	42	2.4
20 d069	*N*-Gly-Lys-cgcgtata-Gln-pTyr-Glu-Glu-Ile-ccaatagc-Lys-Gly-*C* *3′*-GACTGAGGTTATCGT-*5′*	44	8.2
20 d969	*N*-Gly-Lys-cgcgtata-Gln-pTyr-Glu-Glu-Ile-ccaatagc-Lys-Gly-*C* *3′*-AGCGCATAT-G--A-C--T--G-A-GGTTATCGT-*5′*	51	8.8
20 d9′69	*N*-Gly-Lys-cgcgtata-Gln-pTyr-Glu-Glu-Ile-ccaatagc-Lys-Gly-*C* *3′*- AC^{T}CAGA^{T}G-G--A-C--T--G-A-GGTTATCGT-*5′*	52	6.4
20 d909	*N*-Gly-Lys-cgcgtata-Gln-pTyr-Glu-Glu-Ile-ccaatagc-Lys-Gly-*C* *3′*-AGCGCATAT----------GGTTATCGT-*5′*	65	0.4
20 d900 + d009	*N*-Gly-Lys-cgcgtata-Gln-pTyr-Glu-Glu-Ile-ccaatagc-Lys-Gly-*C* *3′*-AGCGCATAT-*5′* *3′*-GGTTATCGT-*5′*	/	4.1
20 p900	*N*-Gly-Lys-cgcgtata-Gln-pTyr-Glu-Glu-Ile-ccaatagc-Lys-Gly-*C* *C*-$Gly-Lys_2$-agcgcatat-Gly_2-*N*	/	0.9
20 p960	*N*-Gly-Lys-cgcgtata-Gln-pTyr-Glu-Glu-Ile-ccaatagc-Lys-Gly-*C* *C*-$Gly-Lys_2$-agcgcatatagtcag-Gly_2-*N*	/	<0.1

[a] PNAs and PNA conjugates were synthesized as C-terminal amides and are represented in lower case and DNA in upper case letters, amino acids are represented in the three letter code. The N- and C-terminal ends of peptides are represented according to IUPAC guidelines, the directionality of PNA conjugates is indicated by marking terminal ends as italicized *N* and *C*. [b] based on IC_{50} measurements and determined by using peptide **17** ($IC_{50} = 3.3$ μM) as a standard.

Several DNA or PNA sequences were designed with an aim to control the SH2 affinity of chimeric molecules **18**–**20** by hybridization. All formed complexes exhibited sigmoidal melting curves indicative of cooperative base pairing (Figure S2) and melting temperatures of $T_m = 34$–$65\,^{\circ}C$ (Table 2). Thus, the formed duplexes provided sufficient stability to maintain structural constraints in protein-binding experiments.

In many cases, DNA hybridization resulted in enhancements of the protein-binding affinity. The largest increases in affinity (almost one order of magnitude) were observed when DNAs **d069** and **d969** were added to hybrid **20** (Table 2). These oligonucleotides contain unpaired nucleotides, which, after hybridization, might be located in the vicinity of the central phosphopeptide. Oligonucleotide **d969** was designed to enable simultaneous hybridization with both PNA arms of hybrid **20**. However, the $T_m = 51\,^{\circ}C$ is significantly below what would be expected for formation of 16 nt PNA–DNA duplexes. The complex that is formed upon addition of DNA **d9′69** has similar thermal stability ($T_m = 52\,^{\circ}C$) though only the C-terminal arm of **20** can be involved in hybridization. This suggests that the hybrid DNA complex **20·d969** presumably adopts an open structure such as **IV**, which is shown in Figure 1 rather than the closed structure **III**. By contrast, the high thermal stability ($T_m = 65\,^{\circ}C$) of the complex that is formed between hybrid **20** and DNA **d909** suggests simultaneous hybridization of both the N- and C-terminal PNA arms. According to this, the

 © 2009 Wiley-VCH Verlag GmbH & Co. KGaA, Weinheim

peptide likely spans a loop to bridge the two hybridized PNA segments (compare **II** in Figure 1). Of note, among the oligonucleotides tested only **d909** was able to induce decreases of the protein affinity upon hybridization. It appears plausible that the decrease in the binding affinity and the increased tendency of the phosphopeptide in **20·d909** to adopt the loop conformation are related. Thus, binding to the Src-SH2 domain might proceed at the cost of an energetic penalty that is required to disrupt seamless base pairing.[52] Though unambiguous evidence for the proposed loop-like peptide structures is lacking, we do note that each of the studied duplexes designed to accommodate a bulged peptide exhibited lower binding affinities than the corresponding PNA–phosphopeptide single strands (compare **1**–**14b** with **1**–**14a** and **20·d909** with **20**).

The exact mechanism that underlies the increases in binding affinity that were observed when oligonucleotides such as **d960**, **d069**, **d969** or **d9′69** were added is less readily explained. The PNA–phosphopeptide hybrids acquire additional negative charge upon binding of DNA. The repulsion between negatively charged PNA–DNA duplex and the negatively charged amino acid residues in the phosphopeptide motif might increase the tendency to adopt extended peptide conformations. In fact, the binding of two, "unconnected" DNA strands (**d900** and **d009**) to PNA–phosphopeptide chimera **20** also resulted in an increase of protein-binding affinity. Furthermore, the additional negative charge near the positively charged phosphotyrosine-binding pocket might provide an additional means for strengthening of the binding interactions. The effect of negative charges became apparent when complementary PNA strands **p900** and **p960** were added to the PNA–phosphopeptide hybrid **20**. PNA has a noncharged backbone. The complex that is formed upon hybridization of DNA **d900** with hybrid **20** had a twofold higher affinity for Src-SH2 than the corresponding PNA-containing complex **20·p900**. Addition of PNA **p960**, which is analogous to DNA **d960**, induced a more than ten-fold decrease of binding activity rather than the fourfold increase of binding affinity that is observed upon addition of DNA **d960**. This decrease of protein affinity upon hybridization with PNA also explains why the difference in affinity between **20** and **20·d909** is not as high as the difference between **8a** and **8b**.

Reversible switching of protein-binding affinity by DNA and RNA hybridization

The hybridization experiments listed in Table 2 exposed PNA–phosphopeptide hybrid **20** as the conjugate that provided the highest differences between two hybridization states. We next explored whether hybridization also allows for reversibility of switching. We envisioned strand-exchange reactions that confer the necessary reorganization in chimera–DNA complexes. It is difficult to displace PNA in a PNA–PNA duplex by DNA.[53] Thus, we chose a strand-exchange reaction that would convert a low-affinity DNA-containing complex such as **20·d909** to an activated complex such as **20·d969**. The PNA segment of hybrid **20** and the deactivating DNA **d909** were shortened in hybrid **21** and DNA **d606**, respectively, to decrease complex stability ($T_m = 39\,^\circ C$ for **21·d606** vs. $60\,^\circ C$ for **20·d909**) and to facilitate replacement by the activating DNA **d969** (Figure 2). The formation of two additional stable base pairs in complex **21·d969** was expected to fuel the exchange of **d606**. Expectedly, the complex **21·d606** was unable to inhibit protein binding of the reference peptide at 1.25 μM concentration. Addition of DNA **d969** resulted in a dramatic increase in fractional inhibition from 0 to 96%, presumably by replacing deactivating DNA **d606** and forming the activated complex **21·d969**.

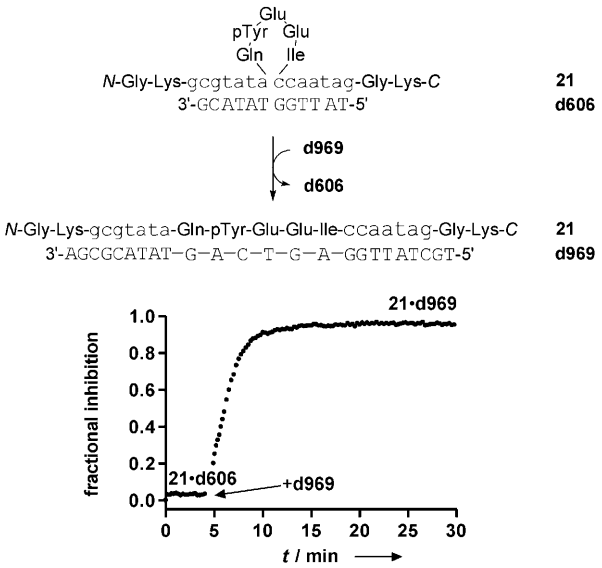

Figure 2. Strand-exchange experiment showing the addition of DNA **d969** to a solution containing Src-SH2 protein, labeled reference peptide FAM-Gly-pTyr-Glu-Glu-Ile-Ala-NH_2, **16** and complex **21·d606**. The arrow indicates the time of DNA addition. Conditions: 1.25 μM **21·d606** in buffer 20 mM NaH_2PO_4, 100 mM NaCl, 2 mM DTT, pH 7.4, 0.1% BSA containing 20 nM **20** and 700 nM GST-Src-SH2, addition of 10 μM DNA **d969** after 4 min.

The preceding switch experiments were based on hybridization reactions with PNA or DNA. The use of RNA-induced switching is appealing because it might allow the reassignment of the function of particular intracellular RNA molecules such as viral RNA or mRNA. In such a scenario, the PNA–peptide hybrid would act as a transducer that couples gene expression with interference in protein–protein recognition. We tested whether nucleic acid mediated switching of PNA–phosphopeptide **21** extends to the use of RNA. The RNA ppp UGC UAU UGG AGU CAG UAU ACG CGA GG_{OH}, **r1169** (segments complementary to **21** are underlined), was prepared by in vitro transcription. The transcription buffer was directly added to hybrid **21** in two aliquots. The sequence of RNA **r1169** was analogous to the sequence of activating DNA **d969**. Thus, it was expected that RNA **r1169** likewise served as an activator. Indeed, each addition step lead to an increase of the fractional inhibition value (Figure 3).

 © 2009 Wiley-VCH Verlag GmbH & Co. KGaA, Weinheim

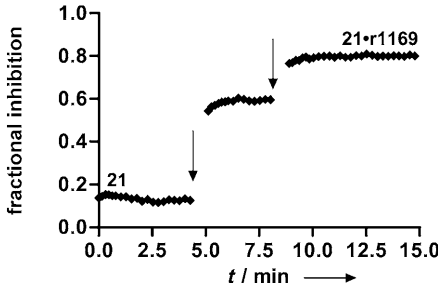

Figure 3. Switching of the inhibitory affinity of chimera **21** by the addition of in vitro transcribed RNA **r1169**. Arrows indicate the point of RNA addition. Conditions: 1.25 μM **21** in buffer 20 mM NaH_2PO_4, 100 mM NaCl, 2 mM DTT, pH 7.4, 0.1% BSA containing 20 nM **16** and 700 nM GST-Src-SH2, direct addition of the in vitro transcription buffer in two aliquots. The RNA concentration was estimated to be approximately 10 μM after addition of the first aliquot, and approximately 20 μM after the addition of the second one.

In vitro kinase reactivation

The inactive, autoinhibited state of Src kinase is induced by phosphorylation of Tyr527, which provides an intramolecular recognition motif for the Src-SH2 domain (Figure 4A). It has been shown that phosphopeptide ligands can compete with pTyr527, which leads to reactivation of the Src kinase.[43] We examined whether the reactivation of the Src kinase by PNA–phosphopeptide chimeras can be controlled by RNA hybridization. We envisaged the use of the chimera–DNA complex **21·d606**, which has a rather low affinity for binding to the Src-SH2 domain. The addition of synthetic RNA 5′-UGC UAU UGG AGU CAG UAU ACG CGA-3′, **r969** was expected to induce a strand-exchange reaction that is driven by the formation of the stable PNA–RNA duplex **21·r969**. This complex allows efficient binding of the phosphopeptide to the Src-SH2 domain. The accompanying disruption of the intramolecular phosphopeptide-SH2 interaction should result in the activation of the enzymatic activity of Src kinase.

An enzyme-linked UV assay developed by Knight et al. was performed to quantify the reactivation of the Src kinase.[54,55] In this assay two coupled enzyme reactions link the production of ADP, which is formed as a byproduct in the kinase reaction, with the oxidation of NADH. The generated NAD^+ was monitored by UV absorption. First, the Src kinase was deactivated upon 30 min preincubation with the Csk kinase.[56] The deactivated Src kinase was added to the kinase reaction buffer. The measured phosphorylation rate provided the 0% reactivation value. Then the phosphorylation, catalyzed by untreated, active Src kinase, was quantified in order to obtain a reference rate for 100% kinase activity. Incubation of the deactivated Src kinase with complex **21·d606** resulted in only 13% recovery of the kinase activity (Figure 4B). In the critical experiment, RNA **r969** was added to the solution of Src kinase and the low-affinity complex **21·d606**. Gratifyingly, a 86% reactivation of kinase activity was obtained.

As a control, Src kinase was incubated with a solution that contained activating RNA **r969** but lacked chimera **21**. This experiment revealed only an insignificant recovery of kinase activity. Thus, reactivation of Src kinase requires PNA–peptide chimera **21** as a transducer. The proof-of-principle results demonstrate for the first time that PNA–peptide chimeras can be used to transduce changes of the concentration of a given RNA molecule to changes of the enzymatic activity of a signal transduction protein.

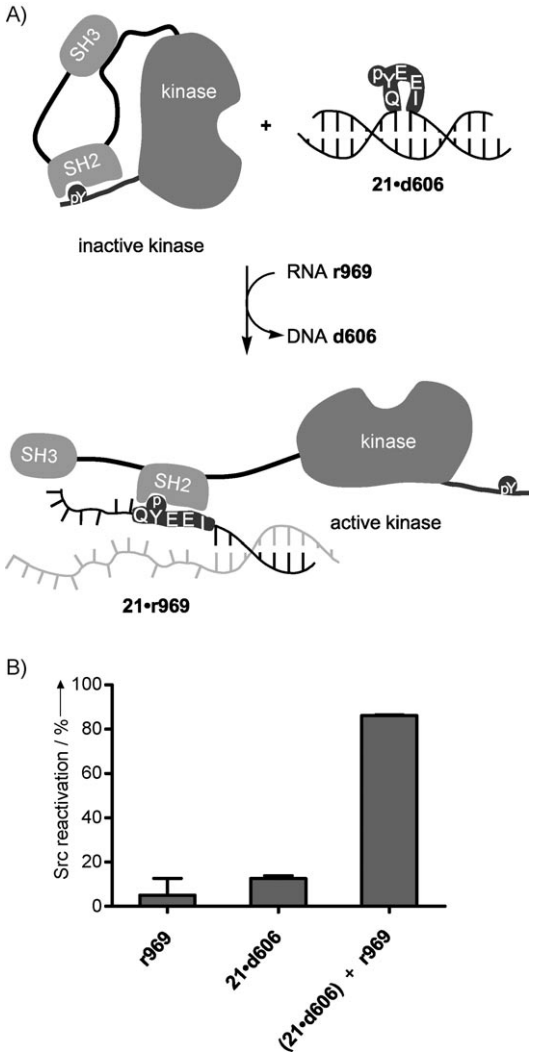

Figure 4. A) Principle of reactivation of Src kinase activity by a PNA–phosphopeptide chimera. The inactive kinase conformation is stabilized by the interaction between pTyr527 and the SH2 domain. Chimera–DNA complex **21·d606** has weak affinity for the Src-SH2 domain. Addition of RNA **r969** triggers the strand-exchange to form activated chimera–RNA complex **21·r969**, which induces activation of the kinase by competing successfully against the pTyr527–SH2 domain interaction. B) Reactivation (in %) of the Src kinase activity by RNA **r969** and deactivated chimera–DNA complex **21·d606** before and after addition of activator RNA **r969**. Conditions: 2 mM substrate peptide **22** (H-Lys-Val-Glu-Lys-Ile-Gly-Glu-Gly-Tyr-Gly-Val-Val-Tyr-Lys-NH_2), 100 mM phosphoenolpyruvate, 30 mM NADH, 5 mM ATP and 5 U pyruvate kinase, 5 U lactate dehydrogenase and 4 nmol Src kinase in buffer (20 mM TRIS, 25 mM $MgCl_2$, 0.2 mM DTT, 20 $\mu g\,mL^{-1}$ BSA, pH 7.5) and 5 μM chimera–DNA complex **21·d606** and 30 μM RNA **r969** when added.

Conclusions

We have shown that both DNA and RNA hybridization can be used to control the bioactivity of the peptide part in PNA–

 © 2009 Wiley-VCH Verlag GmbH & Co. KGaA, Weinheim

phosphopeptide–PNA hybrids. The protein target that was studied, the SH2 domain of Src kinase, binds cognate phosphopeptides, for example, Gln-pTyr-Glu-Glu-Ile, in a linear conformation. Accordingly, each of the studied duplexes that were designed to accommodate bulged peptide structures had lower binding affinity than duplexes that allowed the peptide to adopt extended conformations. Previously, we assumed that simultaneous hybridization of both PNA arms would be required to change the protein affinity.[32] This study suggests that increased binding affinities can be obtained also when only one PNA arm is involved. The different behavior observed in hybridization of the PNA–phosphopeptide conjugate with PNA suggests that the recruitment of negative charges is required to improve binding affinities. Regardless of the mechanism involved, the observed differences in binding affinities spanned almost two orders (>88-fold) of magnitude. It proved feasible to switch from no inhibition to almost quantitative inhibition of the interaction of a protein with a peptide ligand. We demonstrated that the enhancements of the affinity of the hybrid ligand for a protein can be used to regulate the enzymatic activity. The described work provides, to the best of our knowledge, the first example in which RNA was used to trigger the bioactivity of a peptide ligand. We expect that this approach is applicable also to other protein targets required that a high-affinity recognition sequence has been identified.

Experimental Section

Materials: Synthetic DNA oligomers were purchased from BIOTEZ (Berlin, Germany), synthetic RNA oligomers from Invitrogen. In vitro transcription of RNA oligonucleotides has been performed by using a RiboMAX™ express T7 kit (Promega) according to product literature. All aqueous solutions were prepared by using water from an ultrapure water purification system (Membrapure, Bodenheim, Germany). Automated solid-phase synthesis was carried out by using a microscale ResPep-Synthesizer (Intavis AG, Köln, Germany) in microscale columns for PNA synthesis (Intavis AG). Dimethylformamide (DMF), *N*-Methylpyrrolidone (NMP), piperidine and trifluoroacetic acid (TFA) were purchased in peptide synthesis grade and used without further purification. Commercial reagents were obtained from Acros, Fluka, and Sigma and were used without further purifications. PNA monomers were obtained from Applied Biosystems and ASM Research Chemicals (Burgwedel, Germany), standard Fmoc/*t*Bu protected amino acids were purchased from Senn chemicals (Dielsdorf, Switzerland) or NeoMPS (Strasbourg, France). 2-(6-Chloro-1*H*-benzotriazole-1-yl)-1,1,3,3-tetramethylaminium hexafluorophosphate (HCTU) was purchased from Iris Biotech (Marktredwitz, Germany) and the Rink-amide resin (NovaSyn TGR; Novabiochem) as well as the phosphotyrosine building block Fmoc-Tyr(PO(NMe_2)$_2$-OH were obtained from Novabiochem. Detailed synthesis protocol of PNA, PNA–peptide chimeras, and peptides, including full characterization are described in the Supporting Information. Enzymes for the in vitro kinase assay were obtained from Cell Signaling Technology (Src; Danvers, USA), SignalChem (Csk; Richmond, Canada), and Sigma (PK, LDH).

Overexpression and Purification of GST-Src-SH2: The Src-SH2 domain (ggSrc PubMed: aaa70194, 142–246, N243T corresponding to human Src-SH2 145–249, A168P, N224S, T246N) was cloned into the expression vector pGEX-4T1 to produce it as glutathione-S-transferase (GST) fusion protein in *Escherichia coli*. We purified GST-Src-SH2 by glutathione sepharose affinity chromatography, concentration with centrifugal concentrators (Vivaspin 10 kDa MWCO, Viva Science, Sartorius AG, Göttingen, Germany) and size exclusion chromatography (Superdex 75, Pharmacia, Uppsala, Sweden) to obtain a final purity of at least 98%. The purified protein solution was aliquoted and stored at −80 °C after freezing in liquid N_2. Thawed aliquots were stored at 0 °C and used for a maximum of three days.

Fluorescence polarization (anisotropy) experiments: Fluorescence anisotropy experiments were performed on a SPEX Fluoromax 3 fluorescence spectrometer (HORIBA Jobin Yvon, Unterhaching, Germany) that was equipped with a peltier thermostated single-cell holder (set to 25 °C) and automated polarizers. The buffer system was derived from that described by Lynch et al.,[46] but contained BSA instead of the more expensive BGG and consisted of NaH_2PO_4 (20 mM), NaCl (100 mM), DTT (2 mM) and BSA (0.1%) at pH 7.4. Slits were set to yield an intensity of approximately 1.0×10^6 counts with both polarizers set to vertical orientation.

Determination of K_d-values. FAM-labeled chimera was diluted (from a stock solution in 1% Na_2CO_3) in buffer (20 mM NaH_2PO_4, 100 mM NaCl, 2 mM DTT, pH 7.4, 0.1% BSA) to yield a concentration of 20 nM. If desired, the complexing PNA (100 nM final concentration) was added. The resulting solution (1 mL) was titrated with GST-Src-SH2 by using an automated titration system. The resulting anisotropy values were normalized and fitted to the equation for a single site-binding isotherm with receptor depletion (Equation 8.10 in ref. [57]).

Strand-exchange experiment (Figure 2): FAM-labeled reference peptide **16** from a 10 μM stock solution in 1% Na_2CO_3 was added to buffer (0.8 mL, 20 mM NaH_2PO_4, 100 mM NaCl, 2 mM DTT, pH 7.4, 0.1% BSA) to a final concentration of 20 nM. The fluorescence polarization was measured. This value corresponded to the fractional inhibition fi = 1, which was obtained if reference peptide **16** is free in solution. GST-Src-SH2 (from a 1.7 mM stock solution in 20 mM NaH_2PO_4, 100 mM NaCl, 2 mM DTT, pH 7.4) was added to the solution to a final concentration of 700 nM. The measured fluorescence polarization of the quantitatively formed peptide–SH2 complex corresponds to fractional inhibition fi = 0. A preformed complex of chimera **21** and DNA **d606** was added (from a stock solution of 100 μM **21** and 160 μM **d606** in buffer to a final concentration of 1.25 μM **21·d606**. After 2.25 min (10 measurement cycles) data acquisition was paused for 30 s, in this period 10 μM of DNA **d969** was added and the data acquisition was continued after mixing the solution by pipetting it up and down several times.

In vitro kinase assay: First the Src kinase was deactivated upon 30 min preincubation at 30 °C with the Csk kinase.[56] To determine the remaining activity a buffered solution (20 mM TRIS, 25 mM $MgCl_2$, 0.2 mM DTT, 20 μg/mL BSA) that contained Src specific kinase substrate H-Lys-Val-Glu-Lys-Ile-Gly-Glu-Gly-Tyr-Gly-Val-Val-Tyr-Lys-NH_2 (200 μM),[58] ATP (500 μM), phosphoenolpyruvate (1 mM) and NADH (300 μM) as well as pyruvate kinase (PK) and lactate dehydrogenase (LDH) (5 U each) was added to a cuvette, and the reaction was started by adding the Src kinase solution. The kinase activity was assessed by monitoring the optical density at 340 nm and determining the slope at steady-state conditions. After monitoring at steady state conditions for at least 3 min, data acquisition was paused, the compound of interest was added in the desired concentration, and after careful mixing by pipetting the solution up and down several times the data acquisition was continued. To determine the slope for the active Src kinase in another experi-

 © 2009 Wiley-VCH Verlag GmbH & Co. KGaA, Weinheim

ment the kinase was added directly into the assay solution without preincubation with Csk. The reactivation (in %) by the compound that was added was calculated as:[56]

$[(slope_{test} - slope_{Src+Csk})/(slope_{Src} - slope_{Src+Csk})] \times 100$.

Acknowledgements

We acknowledge support from the Volkswagen-Foundation. We are grateful to Lars Hemsath and Patricia Stege (Max-Planck-Institut für Molekulare Physiologie, Dortmund) for expression vectors and help in protein expression.

Keywords: constrained peptides · hybridization · nucleic acids · protein–protein interactions · signal transduction

[1] L. Zhao, J. Chmielewski, *Curr. Opin. Struct. Biol.* **2005**, *15*, 31–34.
[2] L. O. Sillerud, R. S. Larson, *Curr. Protein Pept. Sci.* **2005**, *6*, 151–169.
[3] A. G. Cochran, *Chem. Biol.* **2000**, *7*, R85-R94.
[4] E. Cerasoli, B. K. Sharpe, D. N. Woolfson, *J. Am. Chem. Soc.* **2005**, *127*, 15008–15009.
[5] G. P. Dado, S. H. Gellman, *J. Am. Chem. Soc.* **1993**, *115*, 12609–12610.
[6] L. Gonzalez, J. J. Plecs, T. Alber, *Nat. Struct. Biol.* **1996**, *3*, 510–515.
[7] J. Hentschel, E. Krause, H. G. Börner, *J. Am. Chem. Soc.* **2006**, *128*, 7722–7723.
[8] M. Mutter, R. Hersperger, *Angew. Chem.* **1990**, *102*, 195–197; *Angew. Chem. Int. Ed. Engl.* **1990**, *29*, 185–187.
[9] M. Mutter, R. Gassmann, U. Buttkus, K. H. Altmann, *Angew. Chem.* **1991**, *103*, 1504–1506; *Angew. Chem. Int. Ed. Engl.* **1991**, *30*, 1514–1516.
[10] M. Mutter, A. Chandravarkar, C. Boyat, J. Lopez, S. Dos Santos, B. Mandal, R. Mimna, K. Murat, L. Patiny, L. Saucede, G. Tuchscherer, *Angew. Chem.* **2004**, *116*, 4267–4273; *Angew. Chem. Int. Ed.* **2004**, *43*, 4172–4178.
[11] K. Pagel, T. Vagt, B. Koksch, *Org. Biomol. Chem.* **2005**, *3*, 3843–3850.
[12] K. Pagel, T. Vagt, T. Kohajda, B. Koksch, *Org. Biomol. Chem.* **2005**, *3*, 2500–2502.
[13] K. Pagel, S. C. Wagner, K. Samedov, H. von Berlepsch, C. Bottcher, B. Koksch, *J. Am. Chem. Soc.* **2006**, *128*, 2196–2197.
[14] J. M. Smeenk, M. B. J. Otten, J. Thies, D. A. Tirrell, H. G. Stunnenberg, J. C. M. van Hest, *Angew. Chem.* **2005**, *117*, 2004–2007; *Angew. Chem. Int. Ed.* **2005**, *44*, 1968–1971.
[15] S. G. Zhang, A. Rich, *Proc. Natl. Acad. Sci. USA* **1997**, *94*, 23–28.
[16] G. Mayer, A. Heckel, *Angew. Chem.* **2006**, *118*, 5020–5042; *Angew. Chem. Int. Ed.* **2006**, *45*, 4900–4921.
[17] P. Karrer, R. Keller, G. Szonyi, *Helv. Chim. Acta* **1943**, *26*, 38–50.
[18] I. Willner, *Acc. Chem. Res.* **1997**, *30*, 347–356.
[19] O. Pieroni, A. Fissi, N. Angelini, F. Lenci, *Acc. Chem. Res.* **2001**, *34*, 9–17.
[20] M. Volgraf, P. Gorostiza, R. Numano, R. H. Kramer, E. Y. Isacoff, D. Trauner, *Nat. Chem. Biol.* **2006**, *2*, 47–52.
[21] R. Behrendt, C. Renner, M. Schenk, F. Q. Wang, J. Wachtveitl, D. Oesterhelt, L. Moroder, *Angew. Chem.* **1999**, *111*, 2941–2943; *Angew. Chem. Int. Ed.* **1999**, *38*, 2771–2774.
[22] A. Cattani-Scholz, C. Renner, C. Cabrele, R. Behrendt, D. Oesterhelt, L. Moroder, *Angew. Chem.* **2002**, *114*, 299-302; *Angew. Chem. Int. Ed.* **2002**, *41*, 289–293.
[23] M. Goodman, M. L. Falxa, *J. Am. Chem. Soc.* **1967**, *89*, 3863–3867.
[24] L. Guerrero, O. S. Smart, C. J. Weston, D. C. Burns, G. A. Woolley, R. K. Allemann, *Angew. Chem.* **2005**, *117*, 7956–7960; *Angew. Chem. Int. Ed.* **2005**, *44*, 7778–7782.
[25] J. R. Kumita, O. S. Smart, G. A. Woolley, *Proc. Natl. Acad. Sci. USA* **2000**, *97*, 3803–3808.
[26] C. Renner, L. Moroder, *ChemBioChem* **2006**, *7*, 868–878.
[27] L. Röglin, O. Seitz, *Org. Biomol. Chem.* **2008**, *6*, 3881–3887.
[28] B. Choi, G. Zocchi, Y. Wu, S. Chan, L. J. Perry, *Phys. Rev. Lett.* **2005**, *95*.
[29] B. Choi, G. Zocchi, S. Canale, Y. Wu, S. Chan, L. J. Perry, *Phys. Rev. Lett.* **2005**, *94*.
[30] B. Choi, G. Zocchi, *J. Am. Chem. Soc.* **2006**, *128*, 8541–8548.
[31] B. Choi, G. Zocchi, *Biophys. J.* **2007**, *92*, 1651–1658.
[32] L. Röglin, M. R. Ahmadian, O. Seitz, *Angew. Chem.* **2007**, *119*, 2759–2763; *Angew. Chem. Int. Ed.* **2007**, *46*, 2704–2707.
[33] C. Portela, F. Albericio, R. Eritja, L. Castedo, J. L. Mascarenas, *ChemBioChem* **2007**, *8*, 1110–1114.
[34] P. E. Nielsen, *Curr. Opin. Biotechnol.* **2001**, *12*, 16–20.
[35] O. Seitz, *Angew. Chem.* **2000**, *112*, 3389–3392; *Angew. Chem. Int. Ed.* **2000**, *39*, 3249–3252.
[36] H. Kuhn, V. V. Demidov, J. M. Coull, M. J. Fiandaca, B. D. Gildea, M. D. Frank-Kamenetskii, *J. Am. Chem. Soc.* **2002**, *124*, 1097–1103.
[37] S. M. Thomas, J. S. Brugge, *Annu. Rev. Cell Devel. Biol.* **1997**, *13*, 513–609.
[38] J. Schlessinger, *Cell* **2000**, *103*, 211–225.
[39] T. J. Boggon, M. J. Eck, *Oncogene* **2004**, *23*, 7918–7927.
[40] B. A. Liu, K. Jablonowski, M. Raina, M. Arce, T. Pawson, P. D. Nash, *Mol. Cell* **2006**, *22*, 851–868.
[41] K. Machida, B. J. Mayer, *Biochim. Biophys. Acta Proteins Proteomics* **2005**, *1747*, 1–25.
[42] W. Q. Xu, S. C. Harrison, M. J. Eck, *Nature* **1997**, *385*, 595–602.
[43] X. Q. Liu, S. R. Brodeur, G. Gish, Z. Songyang, L. C. Cantley, A. P. Laudano, T. Pawson, *Oncogene* **1993**, *8*, 1119–1126.
[44] G. Waksman, S. E. Shoelson, N. Pant, D. Cowburn, J. Kuriyan, *Cell* **1993**, *72*, 779–790.
[45] P. Wittung, P. E. Nielsen, O. Buchardt, M. Egholm, B. Nordén, *Nature* **1994**, *368*, 561–563.
[46] B. A. Lynch, K. A. Loiacono, C. L. Tiong, S. E. Adams, I. A. MacNeil, *Anal. Biochem.* **1997**, *247*, 77–82.
[47] J. E. Ladbury, M. Hensmann, G. Panayotou, I. D. Campbell, *Biochemistry* **1996**, *35*, 11062–11069.
[48] P. S. Charifson, L. M. Shewchuk, W. Rocque, C. W. Hummel, S. R. Jordan, C. Mohr, G. J. Pacofsky, M. R. Peel, M. Rodriguez, D. D. Sternbach, T. G. Consler, *Biochemistry* **1997**, *36*, 6283–6293.
[49] T. Gilmer, M. Rodriquez, S. Jordan, R. Crosby, K. Alligood, M. Green, M. Kimery, C. Wagner, D. Kinder, P. Charifson, A. M. Hassell, D. Willard, M. Luther, D. Rusnak, D. D. Sternbach, M. Mehrotra, M. Peel, L. Shampine, R. Davis, J. Robbins, I. R. Patel, D. Kassel, W. Burkhart, M. Moyer, T. Bradshaw, J. Berman, *J. Biol. Chem.* **1994**, *269*, 31711–31719.
[50] T. Ratilainen, A. Holmén, E. Tuite, G. Haaima, L. Christensen, P. E. Nielsen, B. Nordén, *Biochemistry* **1998**, *37*, 12331–12342.
[51] N. H. Nam, R. L. Pitts, G. Q. Sun, S. Sardari, A. Tiemo, M. X. Xie, B. F. Yan, K. Parang, *Bioorg. Med. Chem.* **2004**, *12*, 779–787.
[52] S. Thurley, L. Röglin, O. Seitz, *J. Am. Chem. Soc.* **2007**, *129*, 12693–.
[53] T. N. Grossmann, S. Sasaki, M. Ritzefeld, S. W. Choi, A. Maruyama, O. Seitz, *Bioorg. Med. Chem.* **2008**, *16*, 34–39.
[54] S. C. Barker, D. B. Kassel, D. Weigl, X. Y. Huang, M. A. Luther, W. B. Knight, *Biochemistry* **1995**, *34*, 14843–14851.
[55] W. B. Knight, T. Gilmer, T. Lansing, M. Luther, M. Rodriquez, D. Weigl, *FASEB J.* **1993**, *7*, A1159 A1159.
[56] E. Mandine, V. Jean-Baptiste, W. Vayssiere, D. Gofflo, D. Benard, E. Sarubbi, P. Deprez, R. Baron, G. Superti-Furga, D. Lesuisse, *Biochem. Biophys. Res. Commun.* **2002**, *298*, 185–192.
[57] *Invitrogen Fluorescence Polarization Technical Resource Guide*, 3rd ed., Invitrogen Corporation, Madison, **2004**.
[58] H. C. Cheng, H. Nishio, O. Hatase, S. Ralph, J. H. Wang, *J. Biol. Chem.* **1992**, *267*, 9248–9256.

Received: November 21, 2008

 © 2009 Wiley-VCH Verlag GmbH & Co. KGaA, Weinheim